Check for updates

Analytical and Numerical Stability Analysis of Road Cut Slopes in Garhwal Himalaya, India

Hari Om Singh · Tariq Anwar Ansari ⓘ · T. N. Singh · K. H. Singh

Abstract The rocks of the Himalayan terrain are highly deformed and distorted due to complex geological and tectonics setup. Failures of slopes are always reported along National Highway (NH)-7, in the Uttarakhand Himalayan region, which causes loss of lives, traffic blockage, and destruction of property and also deterioration of the environment gradually. The road cut slope stability analysis of five locations were carried out along NH-7, between Shivpuri to Kaudiyala in Uttarakhand, India. For that a rigorous field investigation was done to collect the geotechnical parameters of slopes and also the potential instability condition of cut slopes were monitored with real time. To know the characteristic of rock mass, the geotechnical data's were studied based on rock mass rating (RMR) and geological strength index (GSI). The kinematics of the blocky (good and fair) rock-mass shows in general wedge, toppling and planar type of failures for different rock slopes. The petrography of representative rock samples was also carried out to see the mineralogical variation in quartzite and phyllitic quartzite. The comparative analysis of different empirical methods for slope stability as slope mass rating (SMR), continuous slope mass rating (Co-SMR), and Chinese slope mass rating (CSMR) shows a decent correlation and revealed that slopes are mostly partially stable. Q_{slope} stability has also been applied to reveal the stability problems and to find out stable slope angle for different slopes. Further to clarify the stability of these slopes, numerical models (LEM and FEM) were applied. The numerical result, (FoS) of different slopes revealed that slopes are stable, critically stable and unstable, with a good agreement between LEM and FEM models. The collective effort of slope stability analysis through analytical and numerical methods will give the better perception to find out the potential remedial measures and optimum slope design.

Keywords Slope stability · SMR · Co-SMR · CSMR · Q_{slope} · Numerical methods

1 Introduction

The state of Uttarakhand in India is such a place in the northern part of Himalayas where every year, millions of pilgrims use roadways to reach their respective shrine and temples such as Rishikesh, Devprayag, Srinagar, Chamoli, Joshimath, Badrinath, and Kedarnath. The Rishikesh–Badrinath (Mana) National Highways (NH-7), is a prime medium for nearly all types of transportation in Uttarakhand, India. Along which the rocks of Garhwal Himalayas are well

H. O. Singh · T. A. Ansari (✉) · T. N. Singh · K. H. Singh
Department of Earth Sciences, Indian Institute of Technology Bombay, Mumbai 400076, India
e-mail: 22tariq@gmail.com

exposed (Valdiya and Bartarya 1989). However, frequent slope failures of the road cut sections pose major hindrance to the socio-economic developments of the region due to lack of alternative railway network and airports (Ansari et al. 2019; Solanki et al. 2019; Gupta et al. 2016; Mahanta et al. 2016).

The failure of slopes in Uttarakhand are common particularly along two zones lying in close proximity of two major tectonic discontinuities i.e. Main Boundary Thrust (MBT) and Main Central Thrust (MCT). Where the neo-tectonic activities along the zones of major thrusts cause a high frequency of slope failure (Valdiya and Bartarya 1989). The state has witnessed several larger landslide events over past two decades e.g. Okhimath landslide along Mandakini valley in 1998 (Sah and Bist 1998), Phata Byung landslide of Rudraprayag district in 2001 (Chaudhary et al. 2010), Budha Kedar landslide in Balganga valley (Sah et al. 2003), Varunawat landslide in 2003 (Gupta and Bist 2004), Agastyamuni landslide in 2005 (Rautela and Pande 2005), landslide in Asi Ganga in 2012 (Martha et al. 2013), Balia Nala landslide and Hill slope instability in Nainital (Kumar et al. 2016; Sah et al. 2018) and Kedarnath tragedy in June 2013 (Vishal et al. 2017) etc. The heavy monsoonal rainfall causes saturation of these slopes, seepage along discontinuity or tension crack and slope undercutting by fluvial erosion, which triggered many landslides in the whole valley (Sati et al. 2011; Singh et al. 2018; Sundriyal et al. 2015).

The cut slopes along the highways in the Himalayan terrain are in general, infested with weak and fractured rock mass with steep weathered slopes, composite discontinuity distribution and overburden of debris mass on weathered slopes (Valdiya and Bartarya 1989; Singh et al. 2013). Slope failures of this region varies from small-scale earth movements to large scale landslides (Varnes 1954, 1996; Cruden and Varnes 1996). The prevailing study of geo-morphological, geotechnical and geo-hydrological conditions shows a combination of processes involve in the earth flow, avalanches, rock fall, rock and debris slide, block topple etc. (Varnes 1954, 1978, 1984; Cruden 1991; Hungr et al. 2014). Where geo-environmental factors such as slope, lithology, terrain units, land cover, soil depth, weathering, aspect, drainage density and lineament density are key factors, which controls the stability of the exposed slope (Hoek and Bray 1991; Wyllie and Mah 2004).

Sati et al. (2011), and Bhandari (2006) claimed that ongoing road widening work, without assessment of geotechnical parameters, ignorance of exact geological structure, defective engineering technique and bad execution of constructions at the base of road leads to increment of slope failures. Due to that several incidents of major or minor landslides have been reported at different cut sections along NH-7 (Sati et al. 2011; Barnard et al. 2001). Fell et al. in 2005 advised that vulnerability analysis of these cut slopes is of great significance for landslide hazard assessment. Recently in the proclaimed area, various methods as analytical, conventional and numerical models were used to analyze these roads cut slopes by researchers as, Ansari et al. (2019); Kundu et al. (2017); Pain et al. (2014); Singh et al. (2014); Siddique et al. (2015) and Siddique (2018); Dudeja et al. (2017); Sarkar et al. (2016); Pandit et al. (2016).

In the present study, road cut sections between Shivpuri to Kaudiyala were chosen along NH-7 in Uttarakhand, for detail rock slope stability analysis. Where five road cut slopes were selected in the Phyllitic quartzite and quartzite rocks of most vulnerable nature. The primary objective includes rock mass characterization (GSI and RMR) and empirical slope stability analysis (SMR, CSMR Co-SMR & Q_{slope}). Where Q_{slope} methods also discuss, to stable the cut slopes by diminishing the slope angle during excavation in more easy and cheap way. Further the numerical simulation with conventional Limit equilibrium method and much advanced Finite element method to evaluate the failure mechanism and factor of safety.

2 Study Area and Field Investigation

The study area is located along the Rishikesh–Badrinath (Mana) National Highway (NH-7), between Shivpuri to Kaudiyala that runs parallel to the Ganga–Alaknanda valley in Garhwal Himalayan, Uttarakhand. It falls on Survey of India toposheet no. 53 J/8, that geographically lies between longitudes of 78° 22′–78° 29′ and latitudes of 30° 07′–30° 04′. The area lies in the northern Lesser Himalayas groups of rocks, where different litho-groups belong to the Infra-Krol formation, lower and upper Tal formation, and Blaini Formation (Valdiya et al. 1975). The rocks are highly affected by major and minor tectonic structures.

The main road cut section of the study area is sandwiched between Saknidhar Thrust (ST) and North Almora Thrust (NAT), and comprised with quartzite and phyllitic quartzite's (Fig. 1). Along the Shivpuri and Kaudiyala Highway, the rocks are intensely fractured, where two to three set of joints can easily found. Most vulnerable nature of five different slopes were chosen for further stability analysis (Fig. 2). During the field investigation, the main aim was to collect the geological and geotechnical data's. The representative rock samples were also collected for experimental study. The field photographs of different cut slopes are shown in Fig. 3 with their extant observations. The geological data of different slopes with their key information are given in Tables 1 and 2.

3 Methodology

The present article discussed the Kinematics and Petrographic study to find out their failure types with their mineralogical variation. The rock mass characteristics were classified based on RMR and GSI techniques and various empirical slope stability methods (SMR, Chinese SMR, continuous SMR, Q_{slope} stability) were adopted to identify their failure potential with remedial measures. Ansari et al. in 2019 has listed a number of empirical methods for stability

Fig. 1 Location map of study area indicating slope locations (1–5)

analysis of slopes, tunnels, mining and underground excavations which are developed by geotechnical, mining and civil engineers. Stability analysis were also carried out using adaptive LEM and advance FEM numerical models to compare the different results with their stability state.

3.1 Kinematic Analysis

The kinematic analysis gives a good indication of stability condition, but it has certain limitations as it does not account for rock and joint properties and external forces like water pressure that has significant effect on stability (Yoon et al. 2002). Kinematic analysis helps us to identify the potential mode of failure based on the angular relationship between discontinuities and the slope surface. This relationship is plotted on an equal angle stereonet to determine mode and direction of failures in computer Program DIPS 6.0.

3.2 Rock Mass Characteristics

RMR_{basic} was initially given by Bieniawski (1979) for the classification of the rock mass. Which uses five parameters such as UCS uniaxial compressive strength (in MPa) of intact rock material, rock quality designation (RQD), the spacing of discontinuities, conditions of discontinuities, and groundwater condition. The RQD was calculated by volumetric joint count (Jv) as in Eq. 1 (Palmström 1982). Where volumetric joint (Jv) was estimated by calculating the joints in cubic meter volume of a rock mass during the field survey.

$$RQD = 115 - 3.3Jv \qquad (1)$$

Hoek & Brown in 1997 suggest that RMR is quite meaningless for weak jointed rock masses (RMR < 25) because of poor RQD value. To overcome such shortcoming of RMR classification, Hoek in 1994 & 1995 established a more efficient and detailed technique of Geological strength index (GSI). Where GSI estimate the reduction in rock mass strength in discrete geological circumstances. Sonmez and Ulusay, in 1999 provided quantitative numerical basis for evaluating GSI by plotting the graph based on two parameters i.e. rock structure and block surface conditions which are described by the following equations.
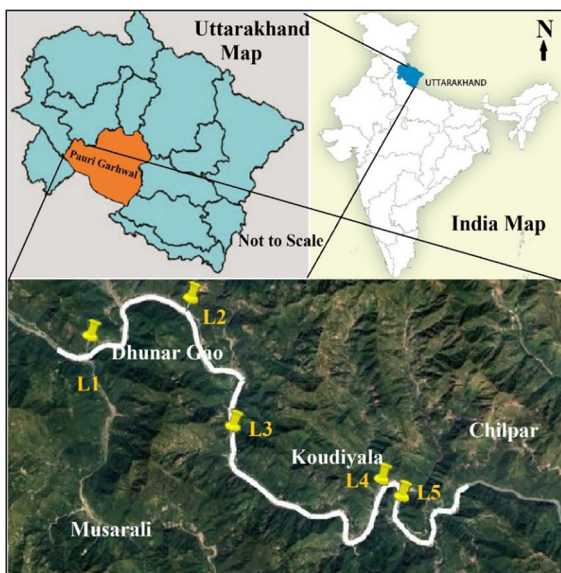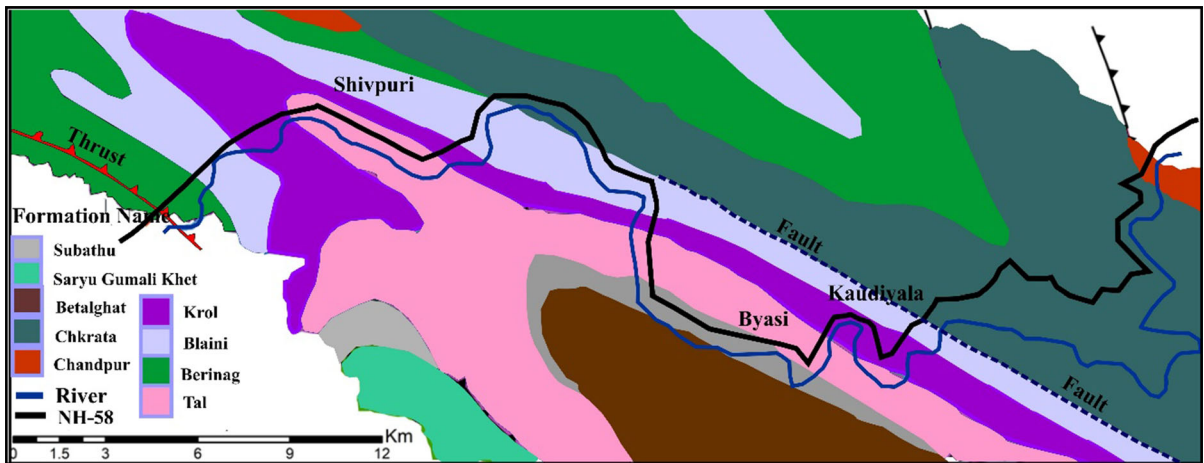
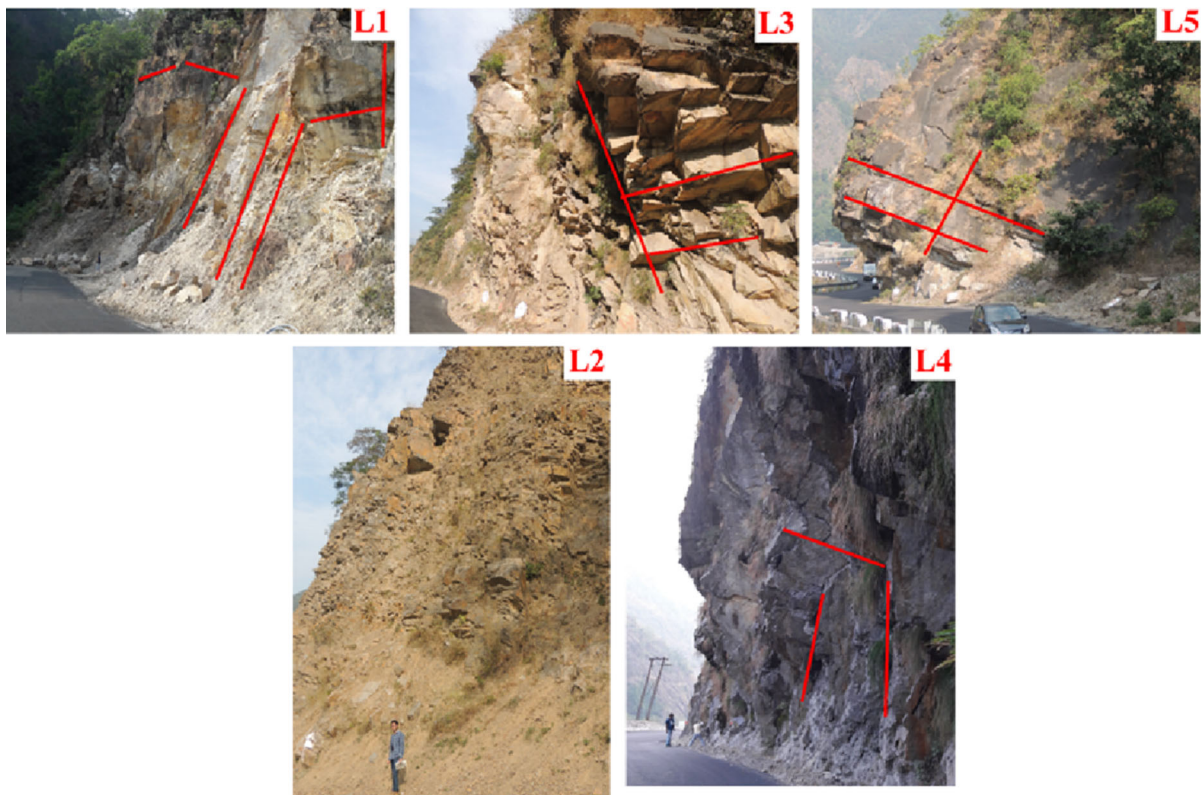**Fig. 2** Geological map of the study area modified after Valdiya (1980)

Fig. 3 Location 1, Planer slope failure; Location 2, Indicate the jointed, blocky slope with the formation of the wedge and block failure; Location 3, Slope dipping upstream direction showing wedge failure; Location 4, Cut slope indicate major joint and overhanging block above highway; Location 5, Two major joint set and formation of potential wedge

$$SR = -17.5 \ln Jv + 79.8 \qquad (2)$$

$$SCR = Rr + Rw + Rf \qquad (3)$$

where Jv = volumetric joint count, Rr = Roughness rating, Rw = Weathering rating, and Rf = Infilling rating.

Table 1 Attributes of discontinuities with their coordinates

Location	Latitude/ longitude	Joint orientation			Slope	Slope height (m)
		J_1	J_2	J_3		
L_1	30° 07′ 13.86″ N 78° 22′ 35.5″ E	65°/N215°	80°/N320°	70°/N82°	70° / N225°	40
L_2	30° 07′ 59.08″ N 78° 24′ 58.51″ E	43°/N35°	75°/N295°	70°/N195°	70° / N236°	55
L_3	30° 05′ 25.47″ N 78° 25′ 59.14″ E	62°/N201°	80°/N298°	28°/ N335°	75° / N240°	65
L_4	30° 04′ 21.60″ N 78° 29′ 30.75″ E	55°/N200°	60°/N300°	75°/N85°	75° / N120°	65
L_5	30° 04′ 00.74″ N 78° 29′ 59.28″ E	58°/N205°	57°/N341°	70°/N100°	68° / N275°	67

3.3 Empirical Methods of Slope Stability

(a) Slope Mass Rating (SMR)

SMR was introduced by Romana (1985) to assess the slope condition, which uses adjustment factors to consider the interrelationship of joint and slope orientation. SMR is calculated from RMRbasic (Bieniawski 1989) by using the formula as shown in Eq. (4).

$$SMR = RMR_{basic} + (F_1 \times F_2 \times F_3) + F_4 \quad (4)$$

where, F1, F2, and F3 are adjustment factors related to joint orientation with respect to slope orientation, and F4 is the correction factor for a method of excavation.

(b) Chinese Slope Mass Rating (CSMR)

CSMR technique is presented by Chen in 1995, where slope height factor (ξ) and discontinuity factor (λ) two more factors were added in the original SMR (Romana 1985). The CSMR are described by the following Eqs. (5).

$$CSMR = \xi\, RMR_{basic} + \lambda\,(F_1 \times F_2 \times F_3) + F_4 \quad (5)$$

where, $\xi = 0.57 + 0.43 \times \frac{80}{H}$ (for slope height > 80 m) or; $\xi = 1$ (for slope height ≤ 80 m).

And λ = 1 for faults of long weak seams filled with clay; 0.8–0.9 for bedding planes of large scale joints with gouge and = 0.7 for joints of tightly interlocked bedding plane.

The rating based on final score of SMR and CSMR are mainly discrete functions and adjustment factors of SMR scheme. Which are somehow on judgment basis and are best defined by experienced geotechnical engineers. Therefore, to facilitate the determination of adjustment factors by less experienced personnel, a

continuous functions proposed by Tomás et al. in 2007, for F₁, F₂, and F₃. The slope designer and geotechnical engineer frequently uses this system to assess the stability of engineered structures in various geological conditions.

(c) Continuous Slope Mass Rating (CoSMR)

CoSMR is given by Tomas et al. 2007, which is reform of discrete SMR technique of Romana (1985). The CoSMR provides unique value of each adjustment factor unlike a range as in SMR and calculated by using the following Eq. (6).

$$CoSMR = RMR_{basic} + (F_1 \times F_2 \times F_3) + F_4 \quad (6)$$

The adjustment factors F_1, F_2 and F_3 are calculated by using the following equations:

$$F_1 = \frac{16}{25} - \frac{3}{500} arctan\left(\frac{1}{10}\left(|A| - 17\right)\right) \quad (7)$$

where, $|A| = |\alpha j - \alpha s|$ for planer failure, $= |\alpha i - \alpha s|$ for wedge failure, $= |\alpha j - \alpha s - 180|$ for toppling failure, and αj, αs, and αi are dip direction of joint, slope and plunge direction of line intersection of two joint planes.

$$F_2 = \frac{9}{16} + \frac{1}{195} arctan\left(\frac{17}{100}(B - 5)\right) \quad (8)$$

where B is equals to dip (βj) of joint for planer and toppling failure, to dip on plunge of line of intersection for wedge failure.

$$F_3 = -30 + \frac{1}{3} \arctan(C); F_3 = -13 - \frac{1}{7}\arctan(C - 120) \quad (9)$$

C is an angular difference of dips of joint and slope (βj−βs) for planer failure. C is difference of dip of plunge of line and dip of slope (βi−βs) for wedge. For

Table 2 Collected geotechnical parameter at studied locations

Location	Rock type/ nature	Joint Parameters	J_1	J_2	J_3	Discontinuity condition	Infilling
L_1	Phyllitic quartzite (Moderately compacted)	Persistence (m)	3–20	3–10	1–6	Good, slightly weathered	Minor sandy and clayey/shale soft < 5 mm
		Aperture(mm)	0.1–1	1–5	0.1–1		
		Average spacing (m)	0.6	0.12	0.0		
		Roughness	Rough	Rough	Rough		
		Water condition	Dry	Dry	Dry		
L_2	Phyllitic quartzite (Loosely compacted)	Persistence (m)	0.5–2	0.1–5	0.2–2	Poor, highly weathered	Clayey/shale soft < 5 mm
		Aperture (mm)	1–5	1–5	0.1–1		
		Average spacing (m)	0.39	0.29	0.071		
		Roughness	Smooth	Slightly rough	Slightly rough		
		Water condition	Dry	Dry	Dry		
L_3	Quartzite (Moderately compacted)	Persistence (m)	3–8	0.5–5	1–4	Good, moderately weathered	Minor sandy material hard < 5 mm
		Aperture(mm)	1–5	0.1–1	1–5		
		Average Spacing (m)	0.1	0.4	0.3		
		Roughness	Rough	Slightly rough	Slightly rough		
		Water condition	Dry	Dry	Dry		
L_4	Phyllitic quartzite (Moderately compacted)	Persistence (m)	10–15	1–5	3–8	Good, moderately weathered, iron stained surface	Clayey/shale soft < 5 mm
		Aperture(mm)	1–5	0.1–1	0.1–1		
		Average spacing (m)	0.5	0.26	0.125		
		Roughness	Slightly rough	Smooth	Slightly rough		
		Water condition	Dry	Dry	Dry		
L_5	Phyllitic quartzite (Moderately compacted)	Persistence (m)	1–3	0.5–3	0.5–2	Fair, moderately weathered	Mix sandy and clayey/shale soft < 5 mm
		Aperture(mm)	0.1–1	< 0.1	0.1–1		
		Average spacing (m)	0.54	0.275	0.18		
		Roughness	Rough	Slightly rough	Slightly rough		
		Water condition	Dry	Dry	Dry		

toppling, C is defined as sum of dip of joint and slope ($\beta j + \beta s$).

The adjustment factor for the method of excavation (F_4) has been fixed empirically as follows:

Natural slopes: $F_4 = + 15$, Presplitting: $F_4 = + 10$; Smooth blasting: $F4 = + 8$; Normal blasting: $F4 = 0$; Deficient blasting: $F_4 = –8$, and Mechanical excavation: $F_4 = 0$.

(d) Q_{slope} Stability

The SMR techniques do not encounter the surficial discontinuity condition and weathering effect in their final score calculation. Therefore, Q_{slope} stability, the modified version of the Q slope classification system (Barton et al. 1974; Barton and Grimstad 2014) has been given by Bar and Barton (2017) to reconsider the additional parameters. The Q_{slope} stability includes numerous additional parameters such as roughness, rock mass structure and frictional characteristics of joint walls or filling materials, strength properties and different geologic and environment condition. It allows the geotechnical engineers to evaluate the stability of excavated rock slopes in the real ground condition. It can help to reduce the slope angle due to local failures and also provide possible adjustments in slope angles according to rock mass conditions during design of road cut slopes and benches. Q_{slope} has the following expression.

$$Q_{slope} = \frac{RQD}{J_n} * \left\{ \frac{J_r}{J_a} \right\}_o * \frac{J_{wice}}{SRF_{slope}} \qquad (10)$$

Where, RQD (Rock quality designation), Jn (Joint sets number), Jr (Joint roughness number), Ja (Joint alteration number), Jr/Ja included discontinuity orientation and wedge adjustment factor (Jr/Ja)o, Jw (ice-wedging effects and tropical rainfall erosion-effects) and SRF_{slope} is strength reduction factor for the slope. Further, SRF_{slope} factor is divided into three parts, namely, SRFa, physical condition number; SRFb, stress-strength number, and SRFc major discontinuity number.

3.4 Numerical Modelling

The conventional limit equilibrium method (LEM) is widely used for slope stability. Which is executed on the basis of finite number of slices and the surface showing minimum factor of safety is called as critical slip surface, it means only a single factor of safety is

applied throughout the whole failure mass (Zhu et al. 2003). It is considered as drawback of LE method, however due to its simplicity (less CPU time) significant number of slope stability are examined over the years (Lin et al. 2014; Singh et al. 2017). The common techniques based on LE principle are the Ordinary/ Fellenius method (1927), Bishop simplified method (1955), Janbu simplified (1968), Janbu corrected (1973), Spencer (1967), Corps of Engineer #1 and #2 (1970), Lowe and Karafiath (1960), and GLE/ Morgenstern- Price (1965). On the basis of previous study carried out by Fredlund and Krahn (1977), Espinoza et al.(1994), Zhu et al. (2003) deduced that position of critical slip surface may deviate in different method and equations of factor of safety with respect to force and moment equilibrium are derived separately.

The finite element method (FEM) has substantial advantage over LE method, where factor of safety is computed without preconceived failure mechanism (Griffiths and Lane 1999). The FEM has been chosen here due to its higher capability in considering geometry and rock mass complexities (Eberhardt 2003; Hammah et al. 2004; Rocscience 2001; Hammouri et al. 2008). The continuum code in FEM model discretize the entire model into numerous small zones, and material property is allocated to each zone and simulated in distinct stress/strain condition (Eberhardt 2003; Stead et al. 2006; Hammah et al. 2005). Mohr–Coulomb failure criterion was used for exact determination of failure envelope in the present modelling of LEM and FEM. Recently, many researchers have attempted numerical methods to determine the stability of cut slopes in the Indian Himalayan region (Mahanta et al. 2016; Siddque et al. 2018; Kanungo et al. 2013; Pain et al. 2014; Gupta et al. 2016; Jamir et al. 2017).

4 Results and Discussion

4.1 Petrography and Kinematics of Different Locations

Photomicrographs of phyllitic quartzite and quartzite were observed under the microscope to find the mineralogical variation, impact of weathering and deformation changes (Fig. 4). The phyllitic quartzite showed that quartz grains were fractured and
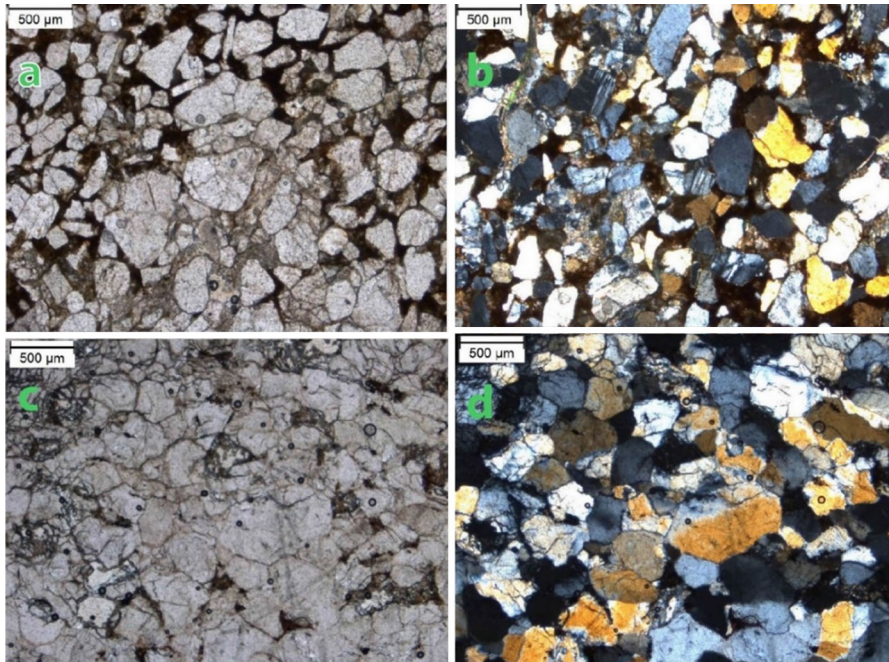
Fig. 4 (Phyllitic Quartzite) **a** PPL & **b** XPL medium grain of well-developed fractured quartz and interstices space was filled by clay band, opaque phases/ ferruginous material; (Quartzite) **c**

PPL & **d** XPL quartz grain possessing inherent networks of fracture with triangular fused grain boundary contact

interstices spaces were filled by opaque phases and ferruginous material (Fig. 4a, b). Where crushed and fused quartz grains with patches of opaque phase and the clay band were formed during initial phase of metamorphism. In the quartzite most of quartz grains have numerous inherent networks of fracture and triangular fused contact which are developed due to high pressure deformation of preexisting lithology. This may be responsible for overall low compressive strength for quartzite (Fig. 4c, d).

For kinematic analysis, the measured structural data of slope & discontinuity planes for all five locations (Table 1) were plotted in the lower hemisphere (equal angle projection) stereograph using Dip 6.0 software. Kinematics of intensely fractured rocks showed prominently the wedge type of failures for all location with planar failure at location 1, and toppling at location 4 & 5 (Fig. 5). The failure probability of different types for different locations are given in the Table 6. In support of kinematics, the wedge formed due to intersection of joints can be clearly seen in the field photograph of different locations (Fig. 3).

4.2 Rock Mass Characteristics

RMR$_{basic}$ was computed from different rock-mass parameters based on field and experimental work. Uniaxial compressive strength (UCS) of representative rock samples was estimated in the lab by using universal testing machine (UTM) as per ISRM suggested methods (2007). Mean values of UCS is shown in Table 3. Rating of different parameters for the RMR$_{basic}$ with their result are shown in Table 4, where locations 1 and 5 are under 'good' category, while locations 2, 3 and 4 are under 'fair' category. RMR$_{basic}$ determination of different vulnerable locations shows that the study area (from Shivpuri to Kaudiyala) have generally good and fair quality of rocks.

GSI value was estimated on the basis of two parameters, i.e. 'structure rating' (SR) and 'surface condition rating' (SCR) as shown in Table 5. The calculated SR and SCR values have been plotted in the quantified GSI chart and red color stars shows GSI value for different locations as shown in Fig. 6 (Sonmez and Ulusay 1999). Estimated GSI value shows that location 1, 2, 4 and 5 have blocky structure
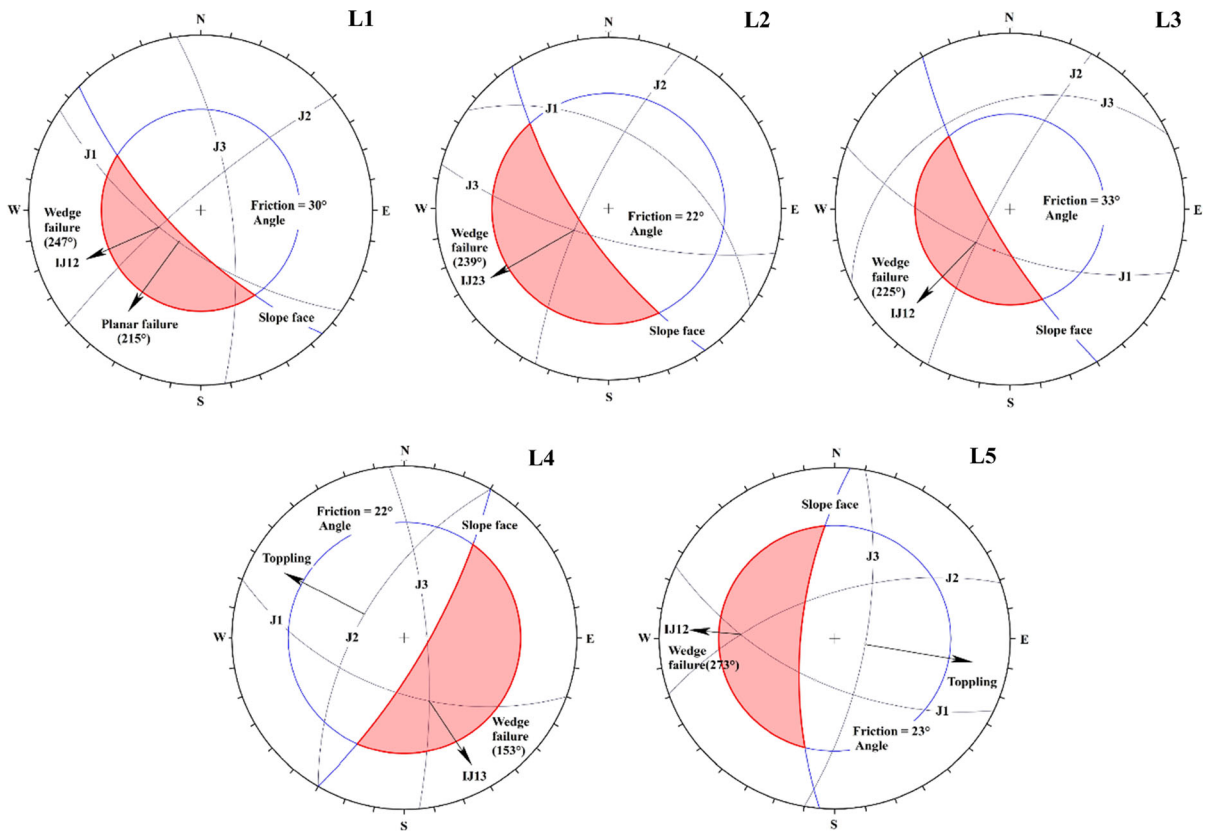
Fig. 5 Kinematic analysis of the jointed rock mass for all the locations (shaded area shows possible failure envelope)

Table 3 Laboratory determined data of representative rocks

Location	σ_{ci}(MPa)	C (MPa)	Φ (°)	E (GPa)
L_1	41.41	0.162	30	19.131
L_2	32.02	0.128	22	14.793
L_3	39.33	0.273	33	14.748
L_4	38.13	0.158	22	17.616
L_5	33.37	0.191	23	15.416

Table 4 Rating of parameters used for the estimation of RMR (Bieniawski 1979)

Location	UCS	RQD	Discontinuity spacing	Condition of discontinuity surface	Groundwater condition	RMR_{basic}	RMR (rock class)
L_1	4	17	12.5	15	15	63.5	Good
L_2	4	8	8	17.5	15	52.5	Fair
L_3	4	13	11.33	16.6	15	59.93	Fair
L_4	4	13	10	17.5	15	52	Fair
L_5	4	17	14	13.3	15	63	Good

Table 5 Different parameters used for the estimation of GSI

Location	Roughness rating (Rr)	Weathering rating (Rw)	Infilling rating (Rf)	SCR (Rr + Rw + Rf)	Jv	SR = −17.5 ln Jv + 79.8	GSI
L1	3	5	2	10	10	39.5	41
L2	3	3	2	8	20.1	27.28	33
L3	3	5	4	12	15.83	31.46	42
L4	3	3	2	8	13.8	33.86	34
L5	3	3	4	10	11.04	37.77	40

with fair surface condition, while location 3 has blocky structure with good surface condition. Quantified GSI value of location 3 was observed to be slightly higher than location 1 & 5 cut slopes due to the compact nature of quartzite. While location 2 and 4 has lower GSI value than other cut slopes due to their heavily jointed nature and surface condition as observed in the field.

4.3 Empirical slope stability analysis

Investigation of slope face by SMR method is likely to give a preliminary assessment of slope stability and providing information about instability mode and required support measures. The adjustment factors F_1, F_2, F_3 have been carefully estimated based on rating of different mode of failures (Kinematic analysis) in each slope and average of adjustment factors has been consider. The value of F_4 has been taken as '−8′ due to poor blasting for excavation to consider the worst case structure (Table 6). SMR is calculated from Eq. (4) using RMR_{basic} for all the locations (Table 6).

According to Romana (1985), location 1, 2, 3 and 5 are in partially stable condition, while location 4 is in stable condition. Different slope locations of normal category may be partially stable but likely to undergo failure depending upon different geological, geotechnical and geo-hydrological (pre and post-monsoon) conditions.

CSMR (Chen 1995) was calculated by using the different parameters accordingly as in Eq. (5)). The result shows that the different locations are in partially stable condition, except location 4, which has CSMR value 40.068 and may consider in unstable state (Table 7).

Similarly for CoSMR, Values of A, B and C can be estimated from the table provided by Romana (1985)

and adjustment factor F_1, F_2, F_3 have been carefully calculated from Eqs. 7, 8 and 9 and value of F_4 is taken as the same as in SMR. The CoSMR values were calculated accordingly as Eq. 6. Results show that the all the locations are partially stable, except the location 4 has 40.96 SMR value, which may be critical between unstable and critical stability class of CoSMR (Table 8).

The parameters required to calculate Q_{slope} stability analysis is given in the Table 9. RQD has been calculated using Eq. (1) and descriptions and ratings for the Q-slope parameters as described in Eq. (10) was assigned using standard rating system provided by Bar and Barton (2017). Estimated Q_{slope} value is shown in Table 10, where maximum value of Q_{slope} is 1.16 for the location 1 and minimum value of 0.049 for the location 4. Q_{slope} stability data chart provided by Bar and Barton (2017) is shown in Fig. 7, where Q_{slope} value and average slope angle in field has been plotted. Q_{slope} stability data chart is categorized into three zone based on slope stability uncertainty, i.e. stable, unstable and partially stable in between stable and unstable zone. Bar and Barton (2017) has also given the formula for different probability of failures based on Q_{slope} value.

Stability of each cut slope in data chart can be seen with red star marks, where slope at location 1 and 5 are critically stable and rest of location are unstable (Fig. 7). From Q_{slope} description, it is possible to reduce the slope angle and design the road cut slope based on probability of failure, during road excavation accordingly. So the same has been incorporated to improve the probability and Q_{slope} value and β angles having probability of failures 1% (PoF = 1%, Slope angle $\beta^0 = 20 \log 10\ Q_{slope} + 65°$) has been plotted in Fig. 7 (Blue star marks). The β angle to stable each
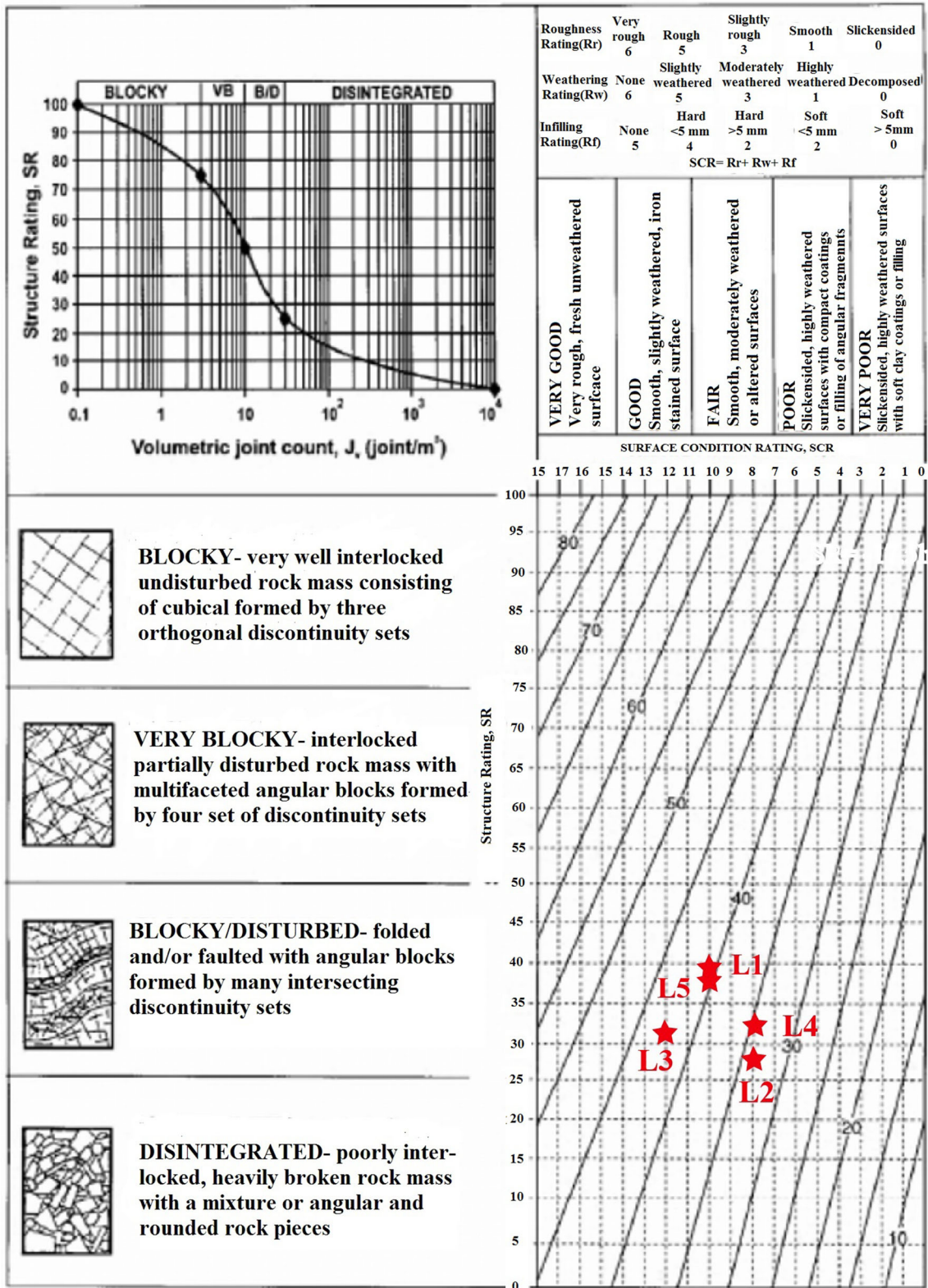
slopes accordingly the failure probability 1% is given in the Table 10.

4.3.1 Comparison of SMR, CoSMR, CSMR and Q_{slope}

As from the SMR, CoSMR, CSMR description and Q_{slope} value for average slope angle from Q_{slope}

stability data chart analysis, the stability problems are explored and correlated for all the locations (Tables 6, 7, 8 and 10). Different SMR techniques, i.e. discrete (SMR and CSMR) and continuous SMR, were compared (Fig. 8). The comparative analysis of SMR techniques and CSMR shows that, maximum variance in rating values was observed 3.7%, which is very slight difference and their stability shows the same result. The comparative analysis between SMR and CoSMR also shows very less variance with a maximum of 5.87%. However, most of the slopes fall under

Table 6 Values of correction factors and SMR for different slopes

Location	F_1	F_2	F_3	F_4	Adjustment factor	RMR_{basic}	SMR	Class/stability	Failure
L_1	0.5	1	−6	−8	−11	63.5	52.5	III/Partially stable	Planer, Wedge
L_2	0.15	1	−6	−8	−8.9	52.5	43.6	III/Partially stable	Wedge
L3	0.15	1	−50	−8	−15.5	59.93	44.43	III/Partially stable	Wedge
L_4	0.43	0.93	−12.5	−8	−12.91	52	39.08	IV/Unstable	Wedge, Toppling
L_5	0.15	0.93	−12.5	−8	−9.73	63	53.26	III/Partially stable	Wedge, Toppling

Table 7 The values of correction factors and CSMR (Chen 1995)

Location	Slope height(m)	ξ	RMRb	ξ. RMRb	λ	F_1	F_2	F_3	F_4	λ.(F1.F2.F3) + F4	CSMR	Class/Stability
L_1	40	1	63.5	63.5	0.8	0.5	1	−6	−8	−10.4	53.1	III/Partially stable
L_2	55	1	52.5	52.5	0.8	0.15	1	−6	−8	−8.72	43.78	III/Partially stable
L_3	65	1	59.93	59.93	0.8	0.15	1	−50	−8	−14	45.93	III/Partially stable
L_4	65	1	52	52	0.8	0.42	0.92	−12.5	−8	−11.93	40.068	IV/Unstable
L_5	67	1	63	63	0.8	0.15	0.92	−12.5	−8	−9.38	53.61	III/Partially stable

Table 8 The values of correction factors and CoSMR (Tomás et al. 2007)

Location	F_1	F_2	F_3	F_4	Adjustment factor	RMR_{basic}	CoSMR	Class/stability
L_1	0.54	0.98	−2.46	−8	−9.31	63.5	54.18	III/Partially stable
L_2	0.15	0.99	−3.77	−8	−8.55	52.5	43.94	III/Partially stable
L_3	0.18	0.98	−57.2	−8	−18.10	59.93	41.82	III/Partially stable
L_4	0.80	0.96	−3.95	−8	−8.91	52	40.96	III/Partially stable
L_5	0.11	0.54	1.17	−8	−7.92	63	55.07	III/Partially stable

Table 9 Estimated Q_{slope} parameters of the studied locations

Location	RQD %	Rating (RQD)	Rating (Jn)	Rating (Jr)	Rating(Ja)	SRFa	SRFb	SRFc	SRF_{slope}	Jwice
L_1	82	17	6	**3**	2	5	2.8	1	8.8	0.5
L_2	48.6	8	9	**3**	8	5	2.6	1	8.6	0.3
L_3	62.76	13	9	**3**	2	5	2.5	4	11.5	0.5
L_4	69.46	13	9	**3**	4	5	2.6	4	11.6	0.1
L_5	78.56	17	6	**3**	4	2.5	2.5	2	7	0.5

Table 10 Estimated Qslope value and slope angle of the studied locations and their stability

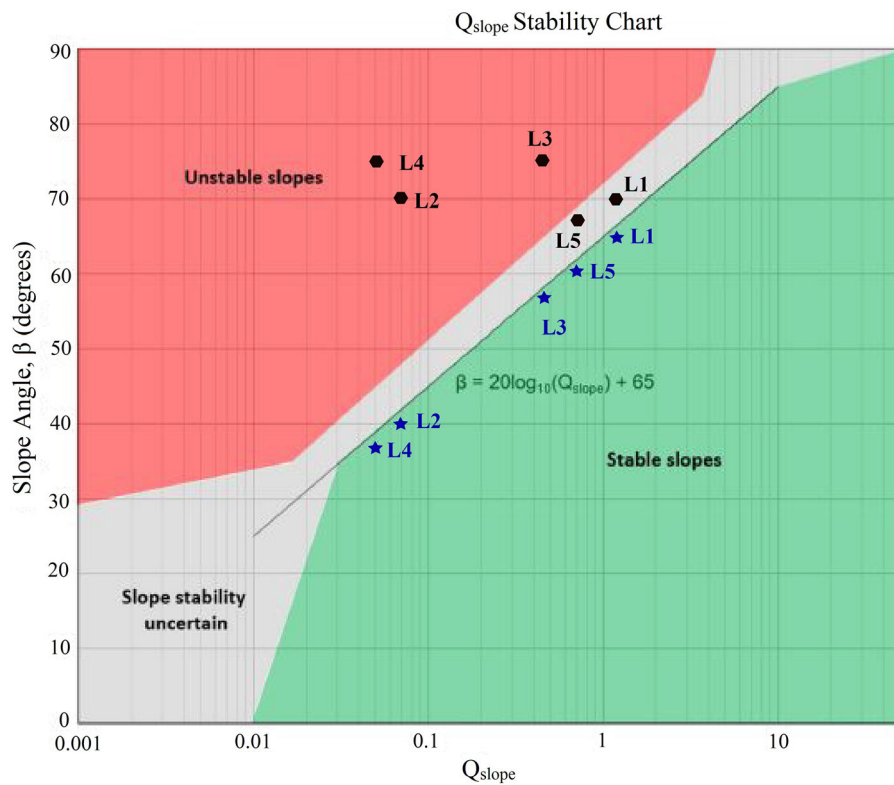| Location	RQD/Jn	Jr/Ja	Jwice/SRF_{slope}	Q_{slope}	Average slope angle (˚)	Slope angle (β^0) for stability	Present stability condition from data chart
L_1	13.66	1.5	0.056	1.16	70	65	Critically stable
L_2	5.4	0.375	0.034	0.07	70	41	Unstable
L_3	6.973	1.5	0.043	0.45	75	54	Unstable
L_4	7.717	0.75	0.008	0.049	75	37	Unstable
L_5	13.093	0.75	0.071	0.70	68	54	Critically stable

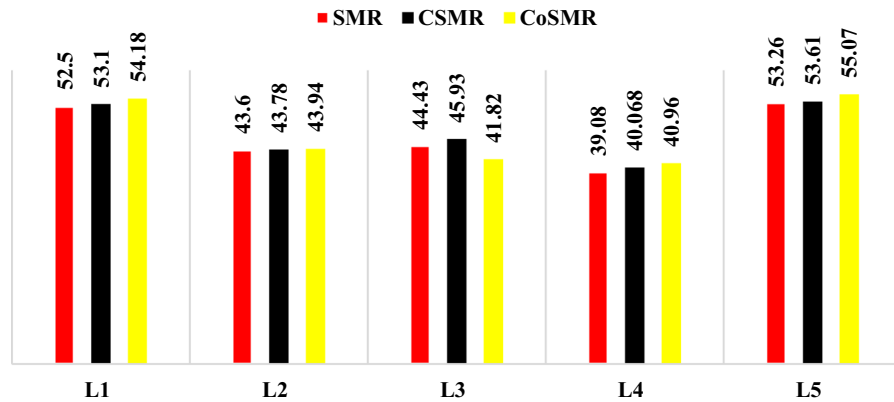**Fig. 7** Data plot of Q_{slope} vs. average slope angle and β angles of the studied locations

Fig. 8 Comparison of various SMR techniques (Original SMR, CoSMR and CSMR)

partially stable condition among SMR, CoSMR and CSMR techniques. Only the location 4 has critical case, because SMR (39.08), CSMR (40.068) and CoSMR (40.98) values lies on the boundary of (partially stable and unstable) different classification techniques. Sardana et al. 2019 has also compared the SMR, CSMR and CoSMR values of road cut slopes along NH-44A, Mizoram, India, which shows almost same type of instability issues in different techniques with slight differences. The Q_{slope} stability analysis from data chart (Fig. 7) shows some difference than other empirical methods for location 2 and 3, while other locations have same type of stability. Ansari et al. (2019) has also calculated the Q_{slope} and SMR technique, where he compared the results of eighteen different rock slopes and showed that most of the result show same type of failure probability in both the techniques.

5 Numerical Modelling

Slope geometry was prepared for all five cut slope sections as observed in the field and then input parameters as in Table 3 were used for further numerical simulation. The quantitative result of numerical simulation in LEM method using Slide V6.0 software, were evaluated. The deterministic factor of safety, and critical slip circles for all cut slopes are shown in Fig. 9.

The FoS values using Mohr- Coulomb criterion were calculated for various LE methods, viz. Ordinary/Fellenius method, Bishop simplified method, Janbu simplified, Janbu corrected, Spencer, Corps of

Engineer #1 and #2, Lowe and Karafiath and GLE/ Morgenstern-Price method (Fig. 10). Where the FoS obtained for Bishop simplified method shows that location 1 (1.36) & 3 (1.31) are fairly stable, location 2 (1.14) & 5 (1.14) are critically stable and location 4 (0.96) is unstable (Fig. 9).

In FEM to determine the Strength Reduction Factor (SRF), Shear Strength Reduction (SSR) technique has been applied to the Mohr- Coulomb criterion using Phase 2 software. FoS results obtained by different methods of LEM were compared with critical SRF of FEM and are presented in Fig. 10. It is clearly observed that, critical SRF i.e. FoS obtained by FEM method has close agreement with Bishop Simplified method and comparatively lower than other LEM methods (Fig. 10). This can be interpreted by the fact that, FEM consider elastic parameters such as Young's modulus and Poisson's ratio in their material properties than LEM. Thus critical SRF calculated by FEM is more authentic and give true results. From FEM analysis the different slopes are critically stable to unstable condition, except location1, which is stable condition (Fig. 11).

Total displacement contour pattern (displayed with deformation vector) has been extracted from FE results to check the extent of possible damage zone (i.e. the zone of failure), their distribution and behaviour across the slope which also depicts deformation intensity and failure mechanism in various parts of the slope. At location 1, the critical SRF is found to be 1.26 which indicates fairly stable condition. The magnitude of displacement contour (Fig. 11) demonstrate that maximum displacement occurs at the top portion of the free face and gradually diminishes
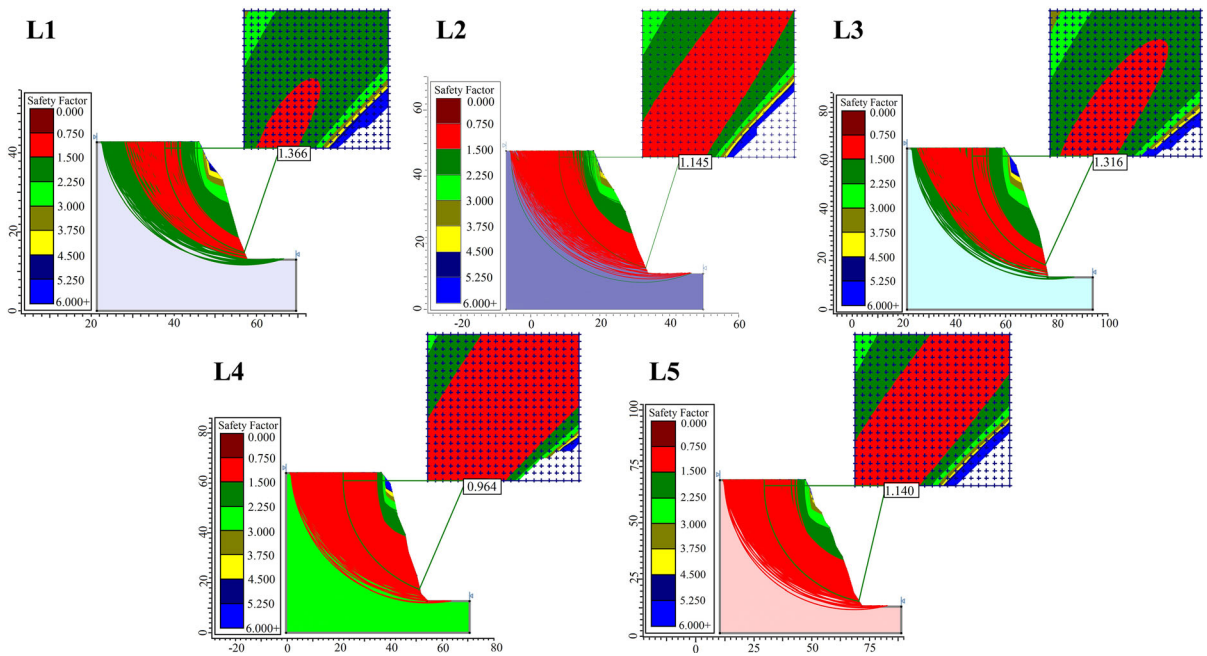
Fig. 9 Limit equilibrium modelling of all studied road cut slopes along NH-7, Uttarakhand, India
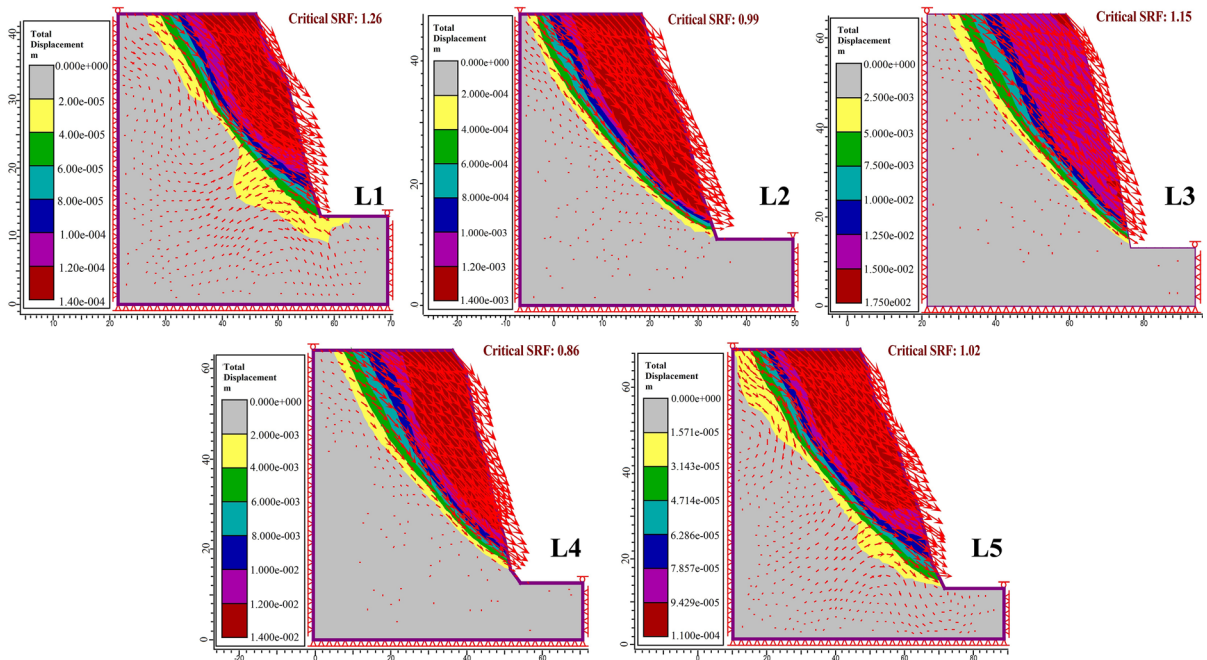

Fig. 10 FoS and Total displacement observed in different Locations (1–5) from FEM analysis

inward to the slope. The overall geometry of slope and discontinuity intersected in such a way that sliding plane daylights on the slope face. From the curvo planer displacement contour, it can be predicted that the slope will undergo wedge and shallow planar failure (which is also predicted from kinematic analysis) and shows the maximum displacement of 1.40e−004 m.
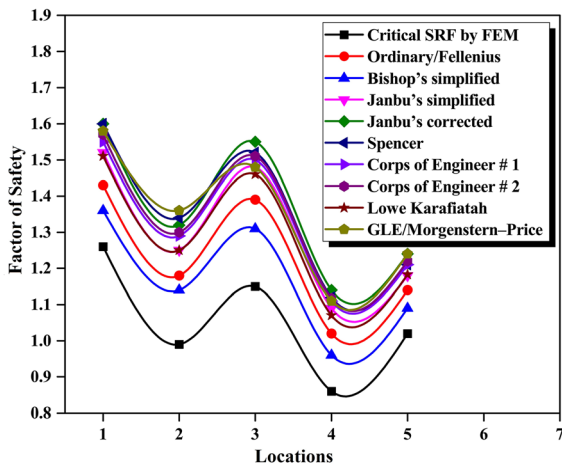
Fig. 11 Comparison of FoS obtained by LEM and FEM methods

At location 2, the critical SRF is found to be 0.99 which indicates unstable condition. Slope is identified as vulnerable to failure especially in rainy season, where many hanging chunks at slope crest usually stuck between larger block and tree roots. Distribution of displacement contour shows the extent of maximum failure zone is mainly confined from crest to toe of the slope (Fig. 11). Based on the nature of distribution and extent of displacement contour, a curvo-planar type of failure can be predicted due to extensive jointing and smaller block size, whereas few active blocks sliding was also seen during field study. Infilling material with water pressure (in rainy season) in joints and fractures reduces stability by increasing the forces that induce sliding (Hoek and Bray, 1991). The impact of gravitational loading at location 2 (H = 55 m) is higher than location 2 (H = 40 m). It is speculated that deeper zone of failure will occur where maximum displacement analyzed in section of $1.40\mathrm{e}{-}003$ m.

At location 3, the critical SRF is found to be 1.15 which indicates fairly stable condition. In the field, slope is very disturbed due to blasting/mechanical excavation and there is rock fall from this cut section and the rock blocks are already getting detached from the slope (Fig. 5). Displacement contours has comparatively lower value than location 2 and location 1 and distributed in slightly curved-planer fashion from peak to toe and show maximum deformation at middle portion of the slope face (Fig. 11). Therefore it is assumed that shallower damage zone across cut section with maximum displacement of

$1.50\mathrm{e}{-}002$ m. Persistence of bedding joint is high at this location and (Eberhardt et al. 2004) recommended that excavation processes continuously disturbed rock masses due to which persistent joints are likely to get exposed and enabling kinematic feasibility in cut slope. At location 4, the critical SRF is found to be 0.86 which indicates highly unstable condition. Displacement contour pattern at this location shows that the most vulnerable part is distributed from apex to middle portion of the free face, which imply possibility of shallow zone of failure. Here, the slope is excavated in such a way that wedges are freely hanging on the roadside (Fig. 3), which is more susceptible to failure especially in monsoon season. Even a small chunk of the block is very threatening to the moving vehicle and human lives. The steepness of slope and extent and nature of distribution of displacement contour show potential for step path failure (Fig. 11). At location 5, the critical SRF is found to be 1.02 which indicates critical instability condition. Damage zone is slightly deeper and distributed from apex to toe of slope (Fig. 11). Steepness and geometry of cut slope, the orientation of discontinuity and apportioning of displacement contour favours wedge failure or toppling.

6 Conclusions

To assess the stability analysis of road cut slopes along NH-7, between Shivpuri to Kaudiyala in Uttarakhand. Five most vulnerable slopes (selected) are studied empirically as well as numerically to find out the failure probability with their attributes. The petrographical studies of representative rock samples of phyllitic quartzite and quartzite's mainly consist quartz, mica, feldspar and clay with some ferruginous minerals. The grains are generally crushed and fused with patches and compositional bands are formed during initial phase of metamorphism. The kinematic analysis showed mostly wedge failure with one or more toppling and planar failure, which has also seen during field visit. The RMR and GSI technique resulted almost same characteristics and revealed that rocks are mostly blocky with fair and good surface condition. The quantitative slope stability analysis using SMR, CSMR and CoSMR techniques for different slopes indicates comparably same result with good agreement, where slopes are partially stable in all

the techniques, except location 4 is unstable in SMR and CSMR techniques. Further to improve the empirical results and to find stable slope angle during exaction, Q_{slope} has been applied. The Q_{slope} analysis shows location 1,2 and 4 has similar type of failure probability as in other empirical methods, while location 2 and 3 are unstable. To stable these slopes β angles have been derived for present Q_{slope} values. As the slopes are partially stable and unstable from empirical slope analysis, further the cost effective numerical models (LEM & FEM) were also applied to enhance the study of slope stability and appropriate remedial measure.

The comparative result of FoS, in LEM and FEM evaluate that different locations are critically stable to unstable, except location 1, which is stable. In LEM method location 2 is also stable. The FoS, result also shows that Bishop Simplified method (LEM) has close agreement to FEM method than other LEM methods. Overall the FEM results and different empirical results evidenced that road cut slopes of Shivpuri to Kaudiyala in Uttarakhand are critically stable to unstable.

References

Ansari TA, Sharma KM, Singh TN (2019) Empirical slope stability assessment along the road corridor NH-7, in the lesser Himalayan. Geotech Geol Eng 37(6):5391–5407

Bar N, Barton N (2017) The Q-slope method for rock slope engineering. Rock Mech Rock Eng 50(12):3307–3322

Barnard PL, Owen LA, Sharma MC, Finkel RC (2001) Natural and human-induced landsliding in the Garhwal Himalaya of northern India. Geomorphology 40(1–2):21–35

Barton NR, Grimstad E (2014) An illustrated guide to the Q-system following 40 years use in tunnelling. Inhouse Publisher, Oslo Retrieved 30 2015

Barton N, Lien R, Lunde J (1974) Engineering classification of rock masses for the design of tunnel support. Rock Mech 6(4):189–236

Bhandari RK (2006) The Indian landslide scenario, strategic issues and action points. In: India disaster management congress, New Delhi pp 29–30

Bieniawski ZT (1979) The geomechanics classification in rock engineering applications. In: 4th ISRM Congress. International Society for rock mechanics and rock engineering

Bieniawski ZT (1989) Engineering rock mass classifications: a complete manual for engineers and geologists in mining, civil, and petroleum engineering. Wiley, Hoboken

Chaudhary S, Gupta V, Sundriyal YP (2010) Surface and subsurface characterization of Byung landslide in Mandakini valley Garhwal Himalaya. Himal Geol 31(2):125–132

Chen Z (1995) Recent developments in slope stability analysis. In: 8th ISRM Congress. International Society for Rock Mechanics and Rock Engineering

Cruden DM (1991) A simple definition of a landslide. Bull Eng Geol Environ 43(1):27–29

Cruden DM, Varnes DJ (1996) Landslides: investigation and mitigation. Chapter 3-Landslide types and processes. Transportation research board special report (247)

Dudeja D, Bhatt SP, Biyani AK (2017) Stability assessment of slide zones in Lesser Himalayan part of Yamunotri pilgrimage route, Uttarakhand, India. Environ Earth Sci 76(1):54

Eberhardt E (2003) Rock slope stability analysis-Utilization of advanced numerical techniques. Earth and Ocean sciences at UBC

Espinoza RD, Bourdeau PL, Muhunthan B (1994) Unified formulation for analysis of slopes with general slip surface. J Geotech Eng 120(7):1185–1204

Fell R, Ho KK, Lacasse S, Leroi E (2005) A framework for landslide risk assessment and management. In: Landslide risk management, CRC Press, pp 13–36

Fredlund DG, Krahn J (1977) Comparison of slope stability methods of analysis. Can Geotech J 14(3):429–439

Griffiths DV, Lane PA (1999) Slope stability analysis by finite elements. Geotechnique 49(3):387–403

Gupta V, Bist KS (2004) The 23 September Varunavat Parvat landslide in Uttarkashi township Uttaranchal, Curr Sci 1600–1605

Gupta V, Bhasin RK, Kaynia AM, Kumar V, Saini AS, Tandon RS, Pabst T (2016) Finite element analysis of failed slope by shear strength reduction technique: a case study for Surabhi Resort Landslide, Mussoorie township, Garhwal Himalaya. Geomatics Nat Hazards Risk 7(5):1677–1690

Hammah RE, Curran H, Yacoub T, Corkum B (2004) Stability analysis of rock slopes using the finite element method

Hammah R, Yacoub T, Corkum B, Curran JH (2005) The shear strength reduction method for the generalized Hoek-Brown criterion

Hammouri NA, Malkawi AI, Yamin MM (2008) Stability analysis of slopes using the finite element method and limiting equilibrium approach. Bull Eng Geol Environ 67(4):471

Hoek E (1994) Strength of rock and rock masses. ISRM News J 2(2):4–16

Hoek E, Bray JW (1991) Rock slope engineering. Elsevier Science Publishing, New York, p 358

Hoek E, Brown ET (1997) Practical estimates of rock mass strength. Int J Rock Mech Min Sci 34(8):1165–1186

Hoek E, Kaiser P K, Bawden WF (1995) Support of underground excavations in hard rock. Rotterdam, Balkema, p 215

Hungr O, Leroueil S, Picarelli L (2014) The Varnes classification of landslide types, an update. Landslides 11(2):167–194

Jamir I, Gupta V, Kumar V, Thong GT (2017) Evaluation of potential surface instability using finite element method in Kharsali Village, Yamuna Valley, Northwest Himalaya. J Mt Sci 14(8):1666–1676

Kanungo DP, Pain A, Sharma S (2013) Finite element modeling approach to assess the stability of debris and rock slopes: a case study from the Indian Himalayas. Nat Hazards 69(1):1–24

Kundu J, Sarkar K, Tripathy A, Singh TN (2017) Qualitative stability assessment of cut slopes along the National Highway-05 around Jhakri area, Himachal Pradesh, India. J Earth Syst Sci 126(8):112

Lin H, Zhong W, Xiong W, Tang W. Slope stability analysis using limit equilibrium method in nonlinear criterion. The Scientific World Journal 2014; 2014.

Mahanta B, Singh HO, Singh PK, Kainthola A, Singh TN (2016) Stability analysis of potential failure zones along NH-305 India. Nat Hazards 83(3):1341–1357

Pain A, Kanungo DP, Sarkar S (2014) Rock slope stability assessment using finite element based modelling–examples from the Indian Himalayas. Geomech Geoeng 9(3):215–230

Palmström A (1982) The volumetric joint count—a useful and simple measure of the degree of rock mass jointing. In: International association of engineering geology. International congress 4, pp 221–228

Pandit K, Sarkar K, Samanta M, Sharma M (2016) Stability analysis and design of slope reinforcement techniques for a Himalayan landslide. In: Recent advances in rock engineering (RARE 2016). Atlantis Press

Rautela P, Pande RK (2005) Traditional inputs in disaster management: the case of Amparav, North India. Int J Environ Stud 62(5):505–515

Rocscience (2001) Phase2 2D finite element program for calculating stresses and estimating support around underground excavations. Toronto

Romana M (1985) New adjustment ratings for application of Bieniawski classification to slopes. In: Proceedings of the international symposium on role of rock mechanics, Zacatecas, Mexico. pp 49–53

Sah MP, Bist KS (1998) Catastrophic mass movement of August 1998 in Okhimath area Garhwal Himalaya. In: Proceeding of international workshop cum training programme on landslide hazard and risk assessment and damage control for sustainable development, New Delhi. pp 259–282

Sah MP, Asthana AK, Rawat BS (2003) Cloud burst of August 10, 2002 and related landslides and debris flows around Budha Kedar (Thati Kathur) in Balganga valley, district Tehri. Himal Geol 24(2):87–101

Sah N, Kumar M, Upadhyay R, Dutt S (2018) Hill slope instability of Nainital City, Kumaun Lesser Himalaya, Uttarakhand, India. J Rock Mech Geotech Eng 10:280–289. https://doi.org/10.1016/j.jrmge.2017.09.011

Sarkar K, Singh AK, Niyogi A, Behera PK, Verma AK, Singh TN (2016) The assessment of slope stability along NH-22 in Rampur-Jhakri Area, Himachal Pradesh. J Geol Soc India 88(3):387–393

Sati SP, Sundriyal YP, Rana N, Dangwal S (2011) Recent landslides in Uttarakhand: nature's fury or human folly. Curr Sci (Bangalore) 100(11):1617–1620

Siddique T, Masroor Alam M, Mondal MEA, Vishal V (2015) Slope mass rating and kinematic analysis of slopes along the national highway-58 near Jonk, Rishikesh, India. J Rock Mech Geotech Eng 7:600–606. https://doi.org/10.1016/j.jrmge.2015.06.007

Singh RP, Dubey CS, Singh SK, Shukla DP, Mishra BK, Tajbakhsh M, Ningthoujam PS, Sharma M, Singh N (2013) A new slope mass rating in mountainous terrain, Jammu and Kashmir Himalayas: application of geophysical technique in slope stability studies. Landslides 10(3):255–265

Singh R, Umrao RK, Singh TN (2014) Stability evaluation of road-cut slopes in the Lesser Himalaya of Uttarakhand, India: conventional and numerical approaches. Bull Eng Geol Environ 73(3):845–857

Singh AK, Kundu J, Sarkar K (2017) Stability analysis of a recurring soil slope failure along NH-5, Himachal Himalaya, India. Nat Hazards. https://doi.org/10.1007/s11069-017-3076-z

Singh AK, Kundu J, Sarkar K (2018) Stability analysis of a recurring soil slope failure along NH-5, Himachal Himalaya India. Nat Hazards 90(2):863–885

Solanki A, Gupta V, Bhakuni SS, Ram P, Joshi M (2019) Geological and geotechnical characterisation of the Khotila landslide in the Dharchula region, NE Kumaun Himalaya. J Earth Syst Sci 128(4):86

Sonmez H, Ulusay R (1999) Modifications to the geological strength index (GSI) and their applicability to stability of slopes. Int J Rock Mech Min Sci 36(6):743–760

Stead D, Eberhardt E, Coggan JS (2006) Developments in the characterization of complex rock slope deformation and failure using numerical modelling techniques. Eng Geol 83(1–3):217–235

Sundriyal YP, Shukla AD, Rana N, Jayangondaperumal R, Srivastava P, Chamyal LS, Sati SP, Juyal N (2015) Terrain response to the extreme rainfall event of June 2013: Evidence from the Alaknanda and Mandakini River Valleys, Garhwal Himalaya India. Episodes 38(3):179–188

Tomás R, Delgado J, Serón JB (2007) Modification of slope mass rating (SMR) by continuous functions. Int J Rock Mech Min Sci 44(7):1062–1069

Valdiya KS (1975) Lithology and age of the Tal Formation in Garhwal, and implication on stratigraphic scheme of Krol Belt in Kumaun Himalaya. Geol Soc India 16(2):119–134

Valdiya KS (1980) The two intracrustal boundary thrusts of the Himalaya. Tectonophysics 66(4):323–348

Valdiya KS, Bartarya SK (1989) Problem of mass-movements in a part of Kumaun Himalaya. Curr Sci 58(9):486–491

Varnes DJ (1954) Landslide types and processes. In: Eckel EB (ed) Landslides and engineering practice, special report 28. Highway research board. National Academy of Science, Washington, DC, pp 20–47

Varnes DJ (1978) Slope movement types and processes. Special Rep 176:11–33

Vishal V, Siddique T, Purohit R, Phophliya MK, Pradhan SP (2017) Hazard assessment in rockfall-prone Himalayan slopes along National Highway-58, India: rating and simulation. Nat Hazards 85(1):487–503

Wyllie DC, Mah CW (2004) Rock Slope Engineering: Civil and Mining, 4th edn. Spon Press, London

Yoon WS, Jeong UJ, Kim JH (2002) Kinematic analysis for sliding failure of multi-faced rock slopes. Eng Geol 67(1–2):51–61

Zhu DY, Lee CF, Jiang HD (2003) Generalised framework of limit equilibrium methods for slope stability analysis. Geotechnique 53:377–395